Journal of the Optical Society of Korea, Vol 5, No. 3, September 2001, pp. 110-116 <Review>

Dark Resonance and Its Potential Applications: High-Resolution Spectroscopy

Byoung Seung Ham*

Center for Quantum Coherence and Ultrafast Information Communications, Electronics and Telecommunications Research Institute, Daejon 305-350, KOREA

(Received May 2, 2001)

Recently observed dark resonance phenomena in solids are reviewed and discussed for potential applications to high-resolution coherence spectroscopy. In an inhomogeneously broadened system, a new type of high-resolution spectroscopy based on electromagnetically induced transparency is demonstrated.

OCIS codes : 190.4720, 270.1670, 300.2570, 300.6240.

I. INTRODUCTION

In an atomic three-level system interacting with two electromagnetic fields, absorption cancellation occurring at certain conditions has drawn much attention to nonlinear and quantum optics. This phenomenon based on quantum coherence and interference can induce tremendous changes in refractive index [1], so that one can control the optical group velocity [2]. The essential feature of this non-absorption phenomenon is dark resonance or population trapping [3,4]. When two resonant laser fields interact with a three-level system, the atom-field interaction induces two superposition states, $|+>$ and $|->$ (see Fig. 1):

$$|+> = [\Omega_1|1> + \Omega_2|2>]/\Omega, \quad (1)$$

$$|-> = [\Omega_2|1> - \Omega_1|2>]/\Omega, \quad (2)$$

where Ω_i is the Rabi frequency of each optical field ω_i and $\Omega^2 = \Omega_1^2 + \Omega_2^2$. Here, it should be noted that the $|->$ state is decoupled from the excited state [4], so the populations in the ground states are pumped into this state and trapped. Due to this coherent population trapping, the system becomes transparent to the applied optical fields.

In 1989, Harris proposed that an optically thick medium can be transparent to the resonant fields [5]. Since then, electromagnetically induced transparency (EIT) has been studied intensively for many potential applications of nonlinear optical processes using atomic gases [6] and solids [7]. The basic physics of EIT is the destructive quantum interference between two absorption pathways to the dressed states, so that the laser fields experience nonabsorption even at the line center. The interaction time must be longer than the excited-state population decay time $(1/\Gamma)$ for the case of the coherent population trapping; the required time for coherent population trapping should be longer than the optical decay time. In EIT, however, it does not need to be because the excitation of the dressed state is only dependent on the applied Rabi frequency Ω when $\Omega > \Gamma$ [8]. This fast coherence excitation opens a door to potential applications of ultrafast optical processes.

Generally, both nonlinear and linear optical susceptibilities are simultaneously increased as the laser frequency tunes closer to the line center. Therefore, nonlinear optical processes should greatly degrade near resonance frequency due to the large absorption. However, such nonlinear optical susceptibility can be increased while the linear susceptibility is reduced. The idea of enhanced nonlinear optical processes is based on the fact that the first-order linear susceptibility

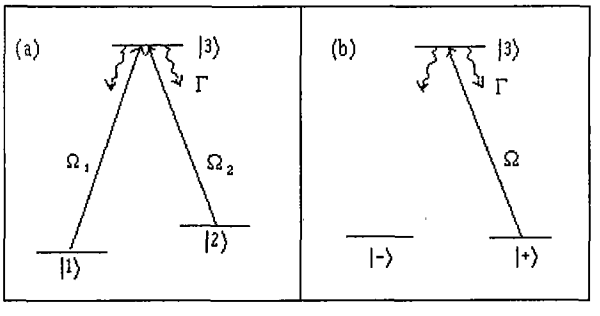

FIG. 1. (a) Bare state basis and (b) coherent state basis.

$Im[\chi^{(1)}]$ is reduced at the line center while the third-order nonlinear susceptibility $Re[\chi^{(3)}]$ is non-zero [9]. Here, four-wave mixing efficiency based on the third nonlinear susceptibility $Re[\chi^{(3)}]$ increases owing to the EIT effect of absorption reduction denoted by first-order linear susceptibility $Im[\chi^{(1)}]$. Recently, enhanced nondegenerate four-wave mixing signals were experimentally demonstrated not only in a single-Λ system [10,11] but also in double-Λ systems of atomic vapors [12], molecular vapors [13], and solids [14].

In this article, observations of EIT in solids are reviewed for potential applications of high-resolution spectroscopy.

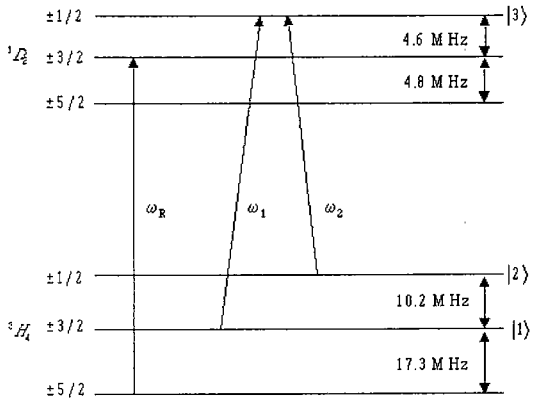

FIG. 2. Partial energy level diagram of Pr:YSO.

II. EIT IN SOLID MEDIA

Although many interesting results of EIT in atomic gas media have been demonstrated, it has had severe restrictions for potential applications because of the diffusive characteristics of the atoms. To overcome such a disadvantage of the atomic media, one may think about solid materials. Of special interest are rare-earth ions doped in crystals. Rare-earth-doped solids have a narrow absorption linewidth (~GHz) and a slow phase decay rate (kHz ~ MHz). Due to the slow decay times (minutes ~ hours) of the hyperfine spin transitions, an optical laser can burn holes easily in the inhomogeneously broadened ground state. This persistent spectral hole-burning effect has been used for ultra-high-density optical data storage [15].

Since the first observation of EIT in solid (Cr^{3+}:Al_2O_3) in 1995 [16], efficient EIT has been demonstrated using a rare-earth Pr^{3+}-doped solid. Several potential applications of EIT were also studied for nonlinear optical processes, such as nondegenerate four-wave mixing [11], enhanced phase conjugation [17], and dynamic optical memory [18]. For spectral modification with laser fields, only spectrally pumped ions can be selected by applying a repump beam [19]. Therefore, the effective number of ions (atoms) can be greatly reduced by the ratio (~10^{-3}) of the laser jitter to the inhomogeneous width so that the EIT condition can be satisfied even at weak laser powers [20]. However, this spectral modification is only possible at certain temperatures, which satisfy the spectral hole-burning phenomena. Thus, the temperature restriction is a major drawback for the implementation of the EIT applications in spectral hole-burning solids.

Fig. 2 shows a partial energy-level diagram of a rare-earth Pr^{3+} (0.05 at.%)-doped Y_2SiO_5 (Pr:YSO). For this work, the relevant optical transition is $^3H_4 \leftrightarrow ^1D_2$, which has a resonance frequency of 606 nm. The optical population decay time T_1 and the phase decay time T_2 are 164 μs and 111 μs, respectively at 1.4K [21]. The optical inhomogeneous width is ~4 GHz. The observed optical homogeneous width increases exponentially as the temperature increases in Pr:YSO, while the spin homogeneous width is almost constant [18]. The ground ($^3H_4$) and the excited ($^1D_2$) states each have three doubly degenerate hyperfine states [21]. The splittings between the hyperfine states of the ground level are 10.2 MHz ($\pm 1/2 \leftrightarrow \pm 3/2$), 17.3 MHz ($\pm 3/2 \leftrightarrow \pm 5/2$), and 27.5 MHz ($\pm 1/2 \leftrightarrow \pm 5/2$) [22]. The ground state population decay time T_1 is ~100 s [22], and spin transverse decay time T_2 for the 10.2 MHz transition is 500 μs at 6 K [18]. The oscillator strength is much weaker ($f \sim 10^{-7}$) than that of most atomic vapors [22]. The small oscillator strength in the Pr-doped crystals is due to the forbidden dipole transitions.

Due to the relatively slow population decay times between the hyperfine states of the ground level, optical spectral hole-burning persists until the populations are redistributed among the three hyperfine states. For the 10.2-MHz transition, the inhomogeneous width of the hyperfine state is measured as 29 kHz by using the rf-optical double resonance technique [14,23]. As the temperature increases, spectral hole burning disappears, so no spectral modification is possible above the critical temperature. Generally, the reason for the disappearance of the spectral hole burning is that the population decay time shortens for the hyperfine transitions. However, such spectral hole burning can also disappear when the optical homogeneous width becomes larger than the hyperfine-state splitting of the ground level: This will be discussed in Fig. 4.

Fig. 3 show EIT observations in Pr:YSO for two cases: (i) persistent spectral hole burning (Fig. 3(a)) and (ii) non-persistent spectral hole burning (Figs. 3(b) and 3(c)). In Fig 3(a), the coupling laser (ω_2) intensity is 90 W/cm^2. At this coupling laser inten-

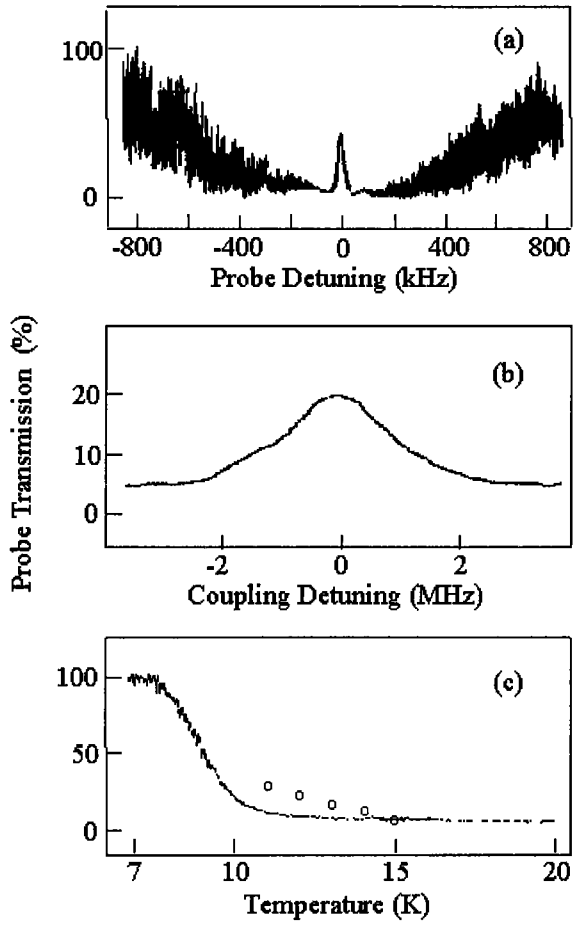

FIG. 3. Probe transmission vs. (a) probe detuning at 2 K, (b) coupling detuning at 12 K, and (c) temperature.

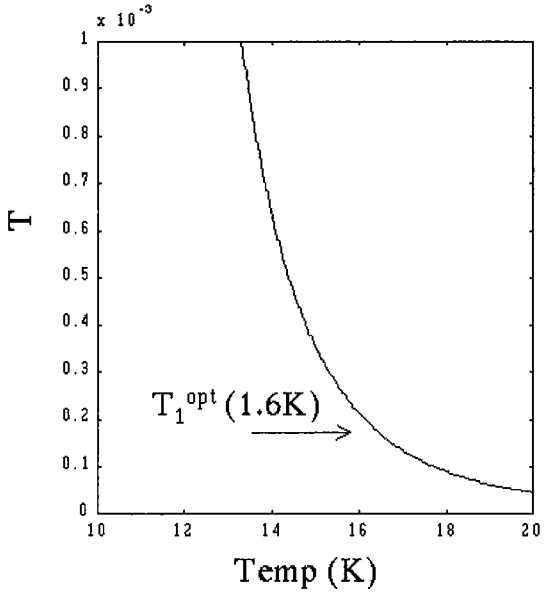

FIG. 4. Numerical simulation of the spin population decay time T_1^{spin} vs. temperature.

sity, the probe absorption reduction is near 40 %. As seen in Fig. 3(a), the spectral width of the EIT window is much smaller than the laser jitter. As the temperature increases, the EIT efficiency decreases, and the EIT window is broadened due to the increased optical homogeneous width. At T = 12K, the absorption reduction of the probe is just 15 % even though the coupling laser intensity is increased up to 1200 W/cm^2 (see Fig. 3(b)). This lower EIT efficiency in Fig. 3(b) can be explained by the increased number of active ions ($\times$1000) comparing with that in Fig. 3(a) and broadened optical homogeneous width; there is no spectral modification in Fig. 3(b).

Fig. 3(c) shows the probe absorption as a function of temperature. For the solid curve the coupling laser is blocked, and the probe intensity is adjusted not to be saturated (over the temperature of the spectral hole burning). The power of the probe beam is 60 μW. Below ~8 K, the sample is nearly transparent to the probe because of the spectral hole burning. The probe transmission rapidly decreases from $\sim$ 100 % to $\sim$ 10 % at 10 K. From the data in Fig. 3(c), the absorption coefficient α is calculated to be ~30/cm at the temperatures of 12 K - 20 K. The open circles in Fig. 3(c) are for the transmission increase owing to EIT when the coupling laser is applied: Fig. 3(b) is for the data (open circle) of Fig. 3(c) at T = 12 K.

Here it should be noted that the spectral width of Fig. 3(b) is close to the laser jitter. Therefore, one may suspect that the absorption decrease in Fig. 3(b) is not due to EIT, but simply due to optical pumping. This will be discussed in Fig. 4.

Fig. 4 shows the population decay time (T_1^{spin}) of the hyperfine states ($|1> \leftrightarrow |2>$ in Fig. 1) as a function of temperature. In Pr:YSO, the decay time is dominated by the Orbach process if the temperature is higher than 3.5K [24]:

$$(T_1^{spin})^{-1} \propto 10^7 \exp(-E/kT), \qquad (3)$$

where E = 85 cm^{-1}, k is the Boltzmann constant, and T is the temperature. As seen in Fig. 4, the spin decay time T_1^{spin} is not faster than the optical decay time T_1^{opt} until T is higher than 16 K. On the other hand, the optical homogeneous width is also rapidly broadened as the temperature increases [18]. Therefore, the disappearance of the persistent spectral hole burning is not due to the faster spin decay time but due to the broadened optical homogeneous width: For laser fields, the hyperfine states can not be distinguished if the optical homogeneous width is larger than the hyperfine splitting. From this discussion, the optical homogeneous width at 12K is deduced to be at least 10.2 MHz, which is one of the hyperfine-state splittings.

III. EIT ENHANCED HIGH-RESOLUTION SPECTROSCOPY

Generally, a narrow bandwidth laser has a big advantage in high-resolution spectroscopy. Therefore, there have been many efforts to develop narrow-bandwidth laser sources. In a three-level system, however, two-photon coherence can alleviate such a laser-bandwidth-dependent spectroscopy because the two-photon coherence spectral width can be much narrower than each laser linewidth. Recently, high-resolution spectroscopy based on EIT was proposed and demonstrated using atomic vapors [25] and solids [14,26].

In this section, counterintuitive laser-jitter-enhanced high-resolution spectroscopy in the three-level solid system of Pr:YSO is discussed. For the present study, the time-resolved four-wave mixing technique is used. EIT-induced phase gratings on the hyperfine states are repeated patterns of the superposition states. Thus, the spectral width of the phase grating should be limited by the spin inhomogeneous width. The spectral linewidth of the four-wave mixing signal, however, can be narrowed in an optically dense medium [14]. The sub-spin-inhomogeneous width was also detected by observing optically excited spin-free-induction-decay signals [26].

Recently, a coherent Raman beat in a Λ-system [27] and phase-correlated four-wave mixing in a V-system[28] were demonstrated using weak-power dichromatic lasers and showed high-resolution spectroscopy for hyperfine states of inhomogenously broadened systems. Especially, the phase-correlated four-wave mixing technique demonstrated a spectroscopic resolution for the hyperfine structures of an excited state which was much higher than that achieved by using the rf-optical double resonance technique [28].

Although jitter free spectroscopy was demonstrated in Ref. [27], the laser jitter should degrade the EIT efficiency in a Λ-system [29]. Thus, the laser jitter should decrease the four-wave mixing efficiency. However, the observed four-wave mixing signal in the present study is nearly unaffected by the laser jitter, and the spectroscopic resolution is even enhanced when the laser linewidth is broader. This counterintuitive laser-jitter-enhanced spectroscopy will be examined with numerical simulations shortly.

For the nondegenerate four-wave mixing scheme, one laser field ω_P is added to the transition of the beam ω_1 of Fig. 1 for two-photon (Raman) coherence detection (not shown). The laser fields of ω_1 and ω_2 in Fig. 1 act as pump beams, which create two-photon ground-state coherence (phase grating) via coherent population trapping or EIT. The laser field ω_P acts as a probe (read) beam, which scatters off the two-

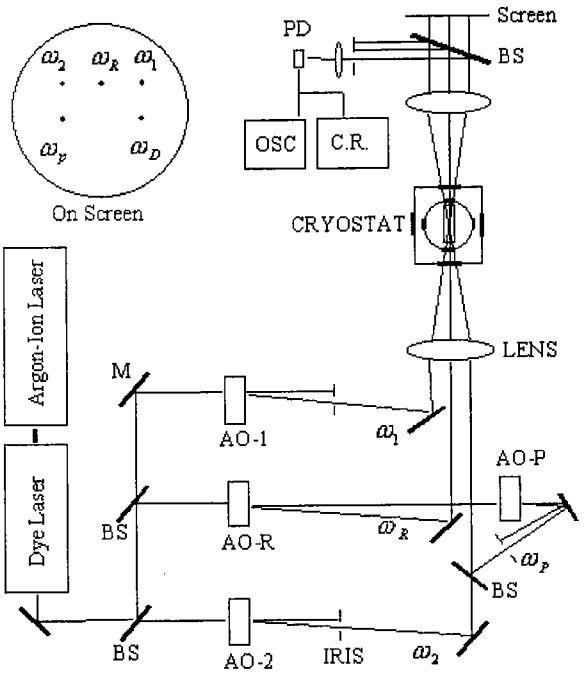

FIG. 5. Schematic of nondegenerate four-wave mixing (AO: Acousto-optic modulator; BS: beam splitter; C.R.: chart recorder; M: mirror; and OSC: oscilloscope). The inset shows the beam positions on the screen.

photon coherence phase gratings created by the pump beams ω_1 and ω_2, and generates a four-wave mix ing signal ω_D satisfying the phase-matching condition $\mathbf{k_D} = \mathbf{k_1} - \mathbf{k_2} + \mathbf{k_P}$. The repump field ω_R is used to provide spectral selectivity in the inhomogeneously broadened system (4 GHz inhomogeneous width). The amount of spectral selectivity depends on the laser jitter.

Fig. 5 shows a schematic of the experimental setup for observing nondegenerate four-wave mixing in Pr:YSO. A frequency stabilized ring dye laser pumped by an Ar-ion laser is used. Acousto-optic modulators driven by frequency synthesizers (PTS 160) are used to make four different coherent laser beams as shown. For the resonant Raman transition, the pump beams ω_1 and ω_2 are downshifted by 60.0 MHz and 70.2 MHz from the laser frequency, respectively. The probe and the repump fields are downshifted from the dye laser output by 70.2 MHz and 47.3 MHz, respectively. All laser beams are linearly polarized and focused into the sample by a 30-cm focal length lens, so the focused beam diameter (e^{-1} in intensity) is ~100 μm. The powers of the pump lasers, ω_1 and ω_2, are 18 mW and 21 mW, respectively. The powers of the probe and the repump lasers, ω_P and ω_R, are 22 mW and 12 mW, respectively. Here, it should be noted that the Rabi frequency is not measured carefully, but the estimated value is ~100 kHz for ~10 m W.

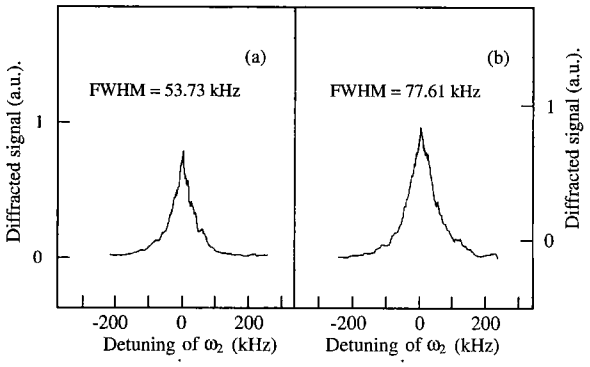

FIG. 6. Four-wave mixing signal ω_D vs. the detuning of ω_2 with (a) unstabilized and (b) stabilized lasers.

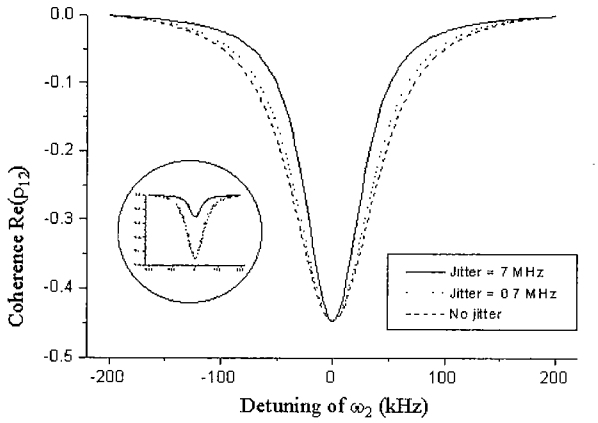

FIG. 7. Numerical calculation of $\mathrm{Re}(\rho_{12})$ vs. two-photon detuning; the optical population (phase) decay rate is 1 (20) kHz for each transition. The Rabi frequency of ω_1 (ω_2) is 200 (200) kHz. The inset is the actual data [26].

To generate laser pulses, rf switches driven by pulse generators are used. The pulse width of the pump and the repump beams is fixed at 1 μs. The probe pulse width is 1 ms and is delayed 2 μs after the end of the pump pulses. A boxcar averager averages 30 samples of the four-wave mixing signal ω_D. The pulse repetition time is long enough ($1/30$ sec $\gg T_2^{spin}$), so the two-photon coherence can not be accumulated. The angle between the pump and the probe beams is about ~70 mrad. The spectral hole-burning crystal, Pr:YSO, is inside a cryostat, and its temperature is kept at 6 K. The size of the crystal is 3.5 mm×4 mm×3 mm. Its optical B-axis is along the 3-mm length, and the laser propagation direction is almost parallel to the optical axis.

Fig. 6 shows the four-wave mixing signals ω_D versus the detuning δ of the pump beam ω_2. For Fig. 6(a), an unstabilized laser whose jitter is ~80 MHz is used. The measured laser jitter is dominated by low frequencies of less than 50 kHz. The spectral width (FWHM) of the diffracted beam ω_D in Fig. 6(a) is 53.7 kHz. In Fig. 6(b), the laser frequency is stabilized down to ~1 MHz. The laser stabilization is achieved by using an external Fabry-Perot cavity locking system. The width (FWHM) of the ω_D in Fig . 6(b) is 77.6 kHz, which is wider than that for an unstabilized laser. Here, it should be noted that both spectral widths in Fig. 6 are power broadened.

To analyze the experimental data in Fig. 6, numerical calculations of density matrix equations for 1 ms pump-pulse are presented. The four-wave mixing signal intensity I_D is proportional to the product of the square of the Raman coherence $\mathrm{Re}(\rho_{12})$ and the probe intensity I_P:

$$I_D \propto \mathrm{Re}(\rho_{12})^2 I_P. \quad (4)$$

This is because the Raman coherence ρ_{12} is proportional to the product of the pump Rabi frequencies (for weak pump beams). Though the Raman coherence ρ_{12} should be position dependent due to linear absorption when the laser beams do not copropagate, the pump energy used in this experiment is enough for saturation. Therefore, the Raman-pump-pulse excited spin coherence ρ_{12} is nearly position invariant, and therefore relation (4) can be used for the four-wave mixing processes: this fact has been experimentally demonstrated [13,17].

Fig. 7 shows Re (ρ_{12}) versus the detuning δ of ω_2 for three different cases of laser jitter. For the calculations, a closed three-level system is assumed. The total number of atoms is fixed to be the same for all three cases so that the coherence Re (ρ_{12}) is weakened as the laser jitter increases (see the inset). Each pump Rabi frequency Ω_i ($i = 1$ or 2) is best guessed to be 200 kHz. To compare the spectral widths of $\mathrm{Re}(\rho_{12})$ with one another, the plots in Fig. 7 are normalized. For this, the dashed curve (with no laser jitter) is chosen as a reference, and the number of atoms for the solid (dotted) curve is increased by a factor of 2.89 (1.04). As seen in Fig. 7, the spectral width of the coherence $\mathrm{Re}(\rho_{12})$ becomes narrower as the laser jitter increases.

Fig. 8 shows Raman coherence $\mathrm{Re}(\rho_{12})$ as functions of both detuning of ω_2 and the atoms' spectral detuning from the absorption line center (resonance of ω_1) for the case of the 7-MHz laser jitter in Fig. 7. Due to the persistent spectral hole-burning, the (effective) optical inhomogeneous width should be determined by the laser jitter. As seen in Fig. 8, off-resonance atoms (1 to 4 MHz with a step of 1 MHz) contribute to the linenarrowing of $\mathrm{Re}(\rho_{12})$ (see Figs. 4 and 5 of Ref. [26] for more detail). Here, it should be noted that the off-resonance atoms should produce lower Raman coherence, too. If the same number of atoms is con-

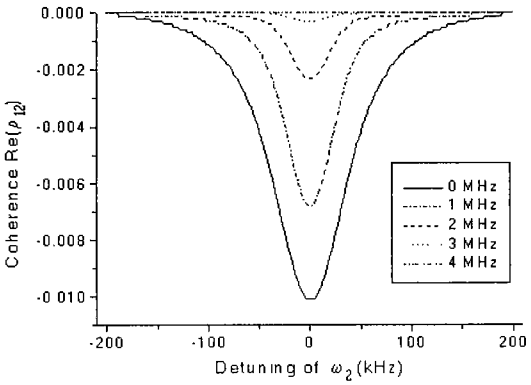

FIG. 8. Numerical calculations of $\mathrm{Re}(\rho_{12})$ vs. detuning of ω_2 for different group of atoms detuned from the line center (see the legend); the Rabi frequency of ω_1 (ω_2) is 200 (200) kHz. All atoms are distributed according to a Gaussian curve having a 7-MHz FWHM.

sidered, the overall four-wave mixing signal should be degraded as the jitter increases (see the inset in Fig. 7). However, in an inhomogeneously broadened persistent spectral hole-burning system, the total number of active atoms is determined by the spectral selection window caused by the laser jitter. Therefore, broader laser jitter should suppress the Raman coherence spectral width while keeping or enhancing overall the four-wave mixing intensity due to the increasing number of atoms in an inhomogeneously broadened persistent spectral-hole-burning medium.

IV. CONCLUSION

EIT observations in a rare-earth-doped persistent spectral-hole-burning solid were reviewed and discussed. Due to the advantage of solid materials over atomic gases in non-atomic diffusion, the observations of EIT in solids have potential applications to nonlinear optical processes, especially, when one is working with images. EIT based high-resolution spectroscopy was also discussed by using resonant Raman pulses and the time-resolved four-wave mixing techniques. The observed laser-jitter-enhanced resolution has potential applications to high-resolution spectroscopy, even when broadband lasers are used.

ACKNOWLEDGMENTS

This work is supported by the Creative Research Initiative Program of the Korean Ministry of Science & Technology.

*Corresponding author : bham@etri.re.kr.

REFERENCES

[1] M. O. Scully, Phys. Rev. Lett. **67**, 1855 (1991).
[2] L. V. Hau, S. E. Harris, Z. Dutton, and C. H. Behroozi, Nature **397**, 594 (1999), and references therein.
[3] G. Alzetta, A. Gozzini, L. Moi, and G. Orrilos, Nuovo Cimento B **36**, 5 (1976).
[4] H. R. Gray, R. M. Whitley, and C. R. Stroud, Jr., Opt. Lett. **3**, 218 (1978); E. Arimondo and G. Orriols, Nuovo Cimento Lett. **17**, 333 (1976).
[5] S. E. Harris, Phys. Rev. Lett. **62**, 1033 (1989).
[6] S. E. Harris, Physics Today **50 (7)**, 36 (1997), and references therein.
[7] B. S. Ham, P. R. Hemmer, M. K. Kim, and M. S. Shahriar, Laser Phys. **9(4)**, 788 (1999), and references therein.
[8] B. S. Ham, M. S. Shahriar, M. K. Kim, and P. R. Hemmer, Phys. Rev. B **58**, R11825 (1998).
[9] S. E. Harris, J. E. Field, and A. Imamoglu, Phys. Rev. Lett. **64**, 1107 (1990).
[10] M. Jain, G. Y. Yin, J. E. Field, and S. E. Harris, Opt. Lett. **18**, 98 (1993)
[11] B. S. Ham, M. S. Shahriar, and P. R. Hemmer, Opt. Lett. **22**, 1138 (1997).
[12] P. R. Hemmer, D. P. Katz, J. Donoghue, M. Cronin-Golomb, M. S. Shahriar, and P. Kumer, Opt. Lett. **20**, 982 (1995); B. Lu, W. H. Burkett, and M. Xiao, Opt. Lett. **23**, 804 (1998).
[13] S. Babin, U. Hinze, E. Tiemann, and B. Wellegehausen, Opt. Lett. **21**, 1186 (1996).
[14] B. S. Ham, M. S. Shahriar, and P. R. Hemmer, Opt. Lett. **24**, 86 (1999).
[15] B. Kohler, S. Bernet, A. Renn, and U. P. Wild, Opt. Lett. **18**, 2144 (1994).
[16] B. S. Ham, Ph.D. Dissertation, "Experimental study of amplification without inversion in ruby," Wayne State University (1995), and published in Phys. Rev. Lett. **79**, 641 (1997).
[17] B. S. Ham, P. R. Hemmer, and M. S. Shahriar, Phys. Rev. A **59**, R2583 (1999).
[18] B. S. Ham, M. S. Shahriar, M. K. Kim, and P. R. Hemmer, Opt. Lett. **22**, 1849 (1997).
[19] B. S. Ham, P. R. Hemmer, and M.S. Shahriar, Opt. Commun. **144**, 227 (1997).
[20] Refer to S. E. Harris and Z. F. Luo, Phys. Rev. A **52**, R928 (1995) for the EIT condition that the photon number should exceed the number of effective atoms in the light path.
[21] K. Holliday, M. Croci, E. Vauthey, and U. P. Wild, Phys. Rev. B **47**, 14741 (1993).
[22] R. W. Equall, R. L. Cone, and R. M. Macfarlane, Phys. Rev. B **52**, 3963 (1995).
[23] L. E. Erickson, Opt. Commun. **21**, 147 (1977).
[24] R. M. Shelby, R. M. Macfarlane, and C. S. Yannoni, Phys. Rev. B **21**, 5004 (1980), and for the parameters in Eq. (3), refer to Ref. 21.

[25] M. D. Lukin, M. Fleischhauer, A. S. Zibrov, H. G. Robinson, V. L. Velichansky, L. Hollberg, and M. O. Scully, Phys. Rev. Lett. **79**, 2959 (1997).
[26] B. S. Ham, P. R. Hemmer, and M. S. Shahriar, Opt. Commun. **164**, 129 (1999).
[27] T. Blasberg and D. Suter, Phys. Rev. B **51**, 6309 (1995).
[28] Y. S. Bai and R. Kachru, Phys. Rev. Lett. **67**, 1859 (1991).
[29] Y-Q. Li and M. Xiao, Phys. Rev. A **51**, 4959 (1995).